

Explainable LP-MPC: Shadow Price Contributions Reveal MV-CV Pairings

Lim C. Siang^{*,**}, Daniel L. O'Connor^{***}

^{*} Burnaby Refinery, Burnaby, BC, Canada

^{**} Georgia Institute of Technology, Atlanta, GA, United States

^{***} Control Consulting Inc., Cascade, MT, United States

Abstract: Large industrial LP-MPC (Linear Program-Model Predictive Control) systems contain tens to hundreds of manipulated variables (MVs) and controlled variables (CVs) for honoring constraints while operating at plant-wide economic optima. The LP is a white-box model, yet for a number of reasons, abnormal behaviors in industrial controllers are often difficult to rationalize. We introduce a novel, post-hoc LP explainability method by recasting the role of shadow prices in the LP solution as an attribution mechanism for MV-CV relationships. The core idea is that CV shadow prices are not just intrinsic properties of the optimal solution, but an aggregate of the cost sensitivities contributed by MVs in enforcing CV constraints, which is then resolved into one-to-one MV-CV pairings using a linear sum assignment solution. The proposed MV-CV pairing framework serves as a practical explainability tool for online LP-MPC systems, enabling practitioners to diagnose suboptimal constraints and verify alignment of the controller's behavior with its original design intent and historical constraints.

Keywords: Model Predictive Control (MPC), Model-Based Control, Dynamic Matrix Control (DMC), LP-MPC, Two-Stage MPC, Linear Programming, Plantwide Control, MV-CV Pairing

1. PROBLEM STATEMENT

A steady-state linear programming (LP) optimizer is commonly used in model-based controllers in the process industries. The LP is used to calculate optimal steady-state targets and the MPC controller is used to dynamically move the plant to the LP targets. The LP calculates manipulated variable (MV) and controlled variable (CV) steady-state targets based on the MPC model, MV and CV limits, and costs. The underlying model predictive control (MPC) algorithm will then find the dynamic move path to these targets. At each execution, the LP-MPC controller calculates new LP targets, and takes a dynamic step towards the LP targets. This two-stage LP-MPC formulation is typically found in commercial packages (Qin and Badgwell, 2003) such as AspenTech DMC3 or Honeywell Profit Suite.

LP-MPC controllers manage complex multivariable interactions to drive plant operations toward economic optima at the boundaries of process and equipment limits. An LP is used to adapt the plant's control strategy in response to changes in operating constraints including feed rate targets, material composition and ambient conditions. These are generally m CV \times n MV non-square controllers designed with more CVs than MVs ($m > n$) to honor all operating limits. To capture benefits, the key degrees of freedom in the process along with all of the constraints must be included. Because MV and CV upper and lower limits are entered as a range, optimization is possible. A critical point of understanding is that each active CV

constraint bounded at its limit will consume a degree of freedom from the unconstrained MVs that are unbounded (Skogestad, 2023). Thus, optimal steady-state operations defined by LP-MPC systems have a $k \times k$ square solution governed by an active constraint set, \mathcal{A} , consisting of the unconstrained MVs and constrained CVs. As MV limits are hit, the size of the square solution in \mathcal{A} is also reduced, as illustrated in Fig. 1.

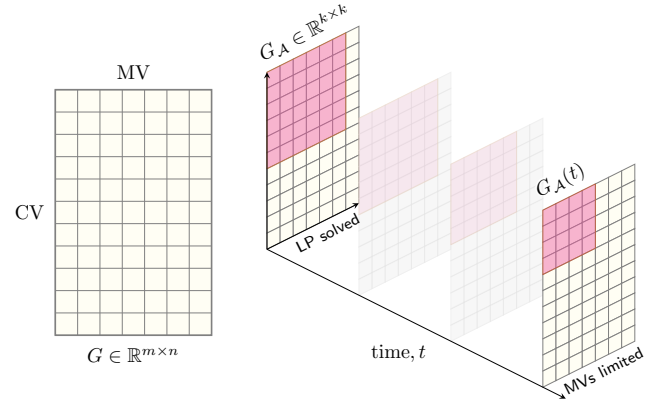


Fig. 1. Evolution of the active constraint set across time $\mathcal{A}(t)$, reducing in size due to constrained MVs.

An important open problem for large-dimensional industrial LP-MPC controllers is addressing the difficulty around explaining the LP solution and understanding why certain active constraint sets emerge during steady-state optimization (Elnawawi et al., 2022). Due to the vertex-driven nature of the LP, even a single disturbance or a minor shift in operating limits can trigger a *basis exchange*

* Corresponding Author: Dan O'Connor (e-mail: doconnor@controlconsulting.com).

(‘pivoting’) in the LP, causing the controller to drop one constraint and pick up another, fundamentally altering the control strategy and the structure of \mathcal{A} . Despite decades of advancements in the theoretical framework of MPC, systematic approaches for reasoning about real-world LP-MPC controllers remain elusive in practice, creating a disconnect between academic MPC developments and the practical needs of engineers and operators in industry.

An unequivocal advantage of white-box LP models is that we know the mathematical structure of the model and we can directly manipulate it. However, simply knowing the LP-MPC model does not mean LP actions based on the model are easily understood. Even for a modest number of MVs and CVs, the combinatorial complexity of MV-CV interactions can make understanding and troubleshooting difficult. For larger controllers, it is often necessary to review large, static displays of numbers to answer questions like “Why is the LP moving a specific MV in a certain direction?” or “Why is the LP cutting feed rate?”. Without a satisfactory answer to rationalize controller actions, operators may adjust MV limits to force a change in behavior, or even switch off the entire controller. These issues represent a critical support gap, and the need for post-hoc explainability tools to troubleshoot controller behavior in an intuitive and self-service manner (Siang et al., 2022).

2. METHODOLOGY

To better understand the targets generated by the LP, we introduce a novel, post-hoc analytical method to explain which unconstrained MV is primarily responsible for enforcing an active CV constraint, defining an MV-CV pair. The shadow price is a basic result from linear programming theory. Although it is typically used in sensitivity analysis, we show that it can also be used for causal attribution purposes. Using it in this manner results in an MV-CV pairing framework that provides a physically interpretable view of active MV-CV interactions. Throughout, we assume that the optimizer is an LP with ‘soft’ CV limits and ‘hard’ MV limits. The LP is formulated to ‘give up’ on less important CVs when the problem is infeasible. At each control interval, the solver returns a solution characterized by an active constraint set, \mathcal{A} of constrained CVs and unconstrained MVs.

We first recall a standard industrial LP-MPC formulation and the associated Karush-Kuhn-Tucker (KKT) optimality conditions. At the optimum, we restrict attention to the active constraint set and derive an expression for the CV shadow prices in terms of the inverse active gain matrix. For the standard industrial formulation where MVs are the decision variables with LP costs assigned, the shadow price of a constrained CV is an aggregate of the cost sensitivities contributed by each unconstrained MV. These sensitivities define a shadow price contribution matrix. When this matrix is corrected for sign and normalized, one-to-one MV-CV pairings can be identified using a linear sum assignment algorithm.

2.1 General LP-MPC Optimizer Formulation

The general form of the LP-MPC problem, as described elsewhere in the literature (Ying and Joseph, 1999; Nikan-

drov and Swartz, 2009), is formulated as a cost minimization problem on incremental MV moves. A brief review of the formulation is presented here.

As part of an MPC control algorithm, a dynamic prediction from the current time to a predicted future ‘steady state’ is maintained for all CVs. At each control interval, the entire CV prediction which includes the prediction at steady state, CV^{ss} , is updated for all MV and disturbance (feedforward) moves which have occurred since the last controller execution, along with the current prediction error. The prediction error is the difference between the current model prediction and the current CV value. In the simplest case, the prediction error is a bias added across the entire prediction horizon and it is implicitly included in the current CV^{ss} value. Now, consider an LP-MPC controller with steady-state gain matrix $G \in \mathbb{R}^{m \times n}$ relating m rows of CVs to n columns of MVs. At each control interval, the steady-state LP optimizer solves for an optimal set of MV moves, $\Delta MV^* \in \mathbb{R}^{n \times 1}$, subject to upper (U) and lower (L) operating limits on the MVs and CVs. The predicted changes in CV steady-state values, $\Delta CV^{ss*} \in \mathbb{R}^{m \times 1}$, are given by $\Delta CV^{ss*} = G \cdot \Delta MV^*$. The possible incremental MV changes based on the current MV values and their limits are $\Delta MV_L = MV_L - MV$ and $\Delta MV_U = MV_U - MV$. The possible incremental CV^{ss} changes based on the current CV^{ss} values and their limits are $\Delta CV_L^{ss} = CV_L - CV^{ss}$ and $\Delta CV_U^{ss} = CV_U - CV^{ss}$.

The overall LP problem has 4 inequality constraints:

$$\begin{aligned} \min_{\Delta MV} \quad & c^T \Delta MV \\ \text{s.t.} \quad & \Delta CV_L^{ss} - G \Delta MV \leq 0, \\ & G \Delta MV - \Delta CV_U^{ss} \leq 0, \\ & \Delta MV_L - \Delta MV \leq 0, \\ & \Delta MV - \Delta MV_U \leq 0. \end{aligned} \quad (1)$$

where $c \in \mathbb{R}^{n \times 1}$ is the cost column vector that represents economic penalties on ΔMV . To analyze the LP optimality conditions, we combine the objective and inequality constraints into the Lagrangian, \mathcal{L} with non-negative shadow prices $\lambda_L, \lambda_U, \mu_L, \mu_U \geq 0$ for each inequality (λ : CV, μ : MV). Applying the KKT conditions for optimality, the stationarity condition states that the gradient of the Lagrangian with respect to the LP decision variables, ΔMV , must vanish at the LP solution:

$$\frac{\partial \mathcal{L}}{\partial \Delta MV} = c - G^T \lambda_L + G^T \lambda_U - \mu_L + \mu_U = 0. \quad (2)$$

Commercial LP-MPC systems report the shadow price for each constrained variable instead of each inequality by collapsing the multipliers into a net shadow price term. Following this practice, we define the net, signed shadow prices as $\lambda \equiv \lambda_L - \lambda_U$ and $\mu \equiv \mu_L - \mu_U$. Algebraic manipulation of (2) yields the stationarity equation in terms of the net shadow prices:

$$c - G^T \lambda - \mu = 0. \quad (3)$$

The shadow prices λ and μ represent the marginal change in the LP objective function if a constraint is relaxed by one unit to allow further incremental MV movement.

2.2 Active Constraint Set Analysis

A key insight is that, at each control interval, the square *active constraint set*, \mathcal{A} governs the control strategy, and

the gain matrix can be partitioned into 4 sub-matrices, G_A, G_B, G_C and G_D , based on each variable's constraint.

$$G = \begin{matrix} & \begin{matrix} MV_u & MV_c \end{matrix} \\ \begin{matrix} CV_c \\ CV_u \end{matrix} & \left[\begin{array}{c|c} G_A & G_B \\ \hline G_C & G_D \end{array} \right] \end{matrix} \quad (4)$$

MV_u represents unconstrained MVs and the degrees of freedom available to hold constrained CVs, CV_c at their limits. MV_c are constrained MVs that are saturated and not useful for controlling any CVs, and CV_u are unconstrained CVs floating between limits. Knowing $G_A \in \mathbb{R}^{k \times k}$ where $k \equiv |CV_c| = |MV_u|$, allows us to impose further restrictions on the net stationarity equation in (3) by taking rows that only correspond to the unconstrained MVs for every term. Due to complementary slackness, the unconstrained variables have zero shadow prices, $\mu_i = 0$ and $\lambda_j = 0$. This analysis yields the restricted stationarity equation for the active constraint set: $c_u - G_A^T \lambda = 0$ in column-vector form where $c_u \in \mathbb{R}^{k \times 1}$ and $\lambda \in \mathbb{R}^{k \times 1}$. Transposing this result using $(AB)^T = B^T A^T$, we see equivalently in row-vector form $\lambda^T G_A = c_u^T$.

Conceptually, the LP optimizer is driving the solution in \mathcal{A} in the cost minimization direction, represented by the cost vector c_u , until it reaches an equilibrium due to opposing forces, which are the penalties of CV constraint violation, represented by $\lambda^T G_A$, as shown in Fig. 2. From a linear programming theory perspective, at optimality, G_A is the *basis matrix* in the simplex algorithm and the shadow prices are the dual solution.

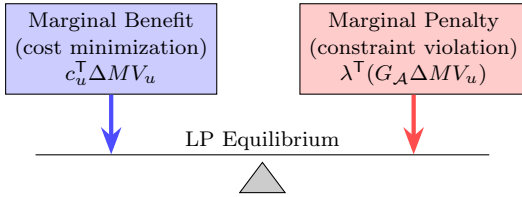


Fig. 2. LP equilibrium balancing benefit of MV_u cost minimization with penalty of CV_c constraint violation.

In industrial LP-MPC controllers with well-conditioned gain matrices, and CVs formulated as ‘soft constraints’ to handle LP infeasibilities, G_A is square and invertible in the LP solution, allowing us to express the CV shadow prices analytically as a function of the inverse gain matrix:

$$\lambda^T = c_u^T G_A^{-1} \quad (5)$$

The inverse active gain submatrix, G_A^{-1} , with MVs as rows and CVs as columns, uncovers any indirect relationships between MV and CVs that are not present in the open-loop gain matrix, G , due to the LP solution that's driving MV_u to control CV_c at their limits.

2.3 Shadow Price Contributions by MVs

From (5), we define a *shadow price contribution matrix* W that recovers, in unreduced form, the element-wise cost-weighted MV contributions before they are column-wise aggregated into the observed CV shadow prices from the LP solution:

$$W = \text{diag}(c_u) \cdot G_A^{-1} \quad (6)$$

W explains the marginal cost of individual MV movements responsible for enforcing CV constraints in the active con-

straint set \mathcal{A} . Each w_{ij} element represents the contribution of MV_i to the shadow price λ_j of CV_j , which is a weighted sum along each CV column in the W matrix, $\lambda_j = \sum_{i=1}^k w_{ij}$ as illustrated in Fig. 3.

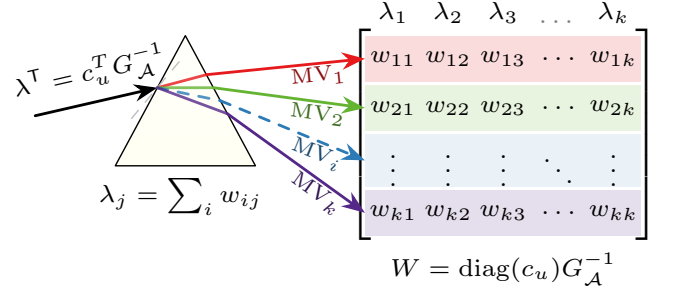


Fig. 3. Shadow price broken down by MV contributions

The physical interpretation of W is complicated by the directional asymmetry and sign patterns on the CV shadow prices λ , as described earlier in (5). If $\lambda_j < 0$, the CV upper bound is constrained. For a consistent interpretation in alignment with the cost-reducing direction of the LP objective, we apply a sign-adjusted correction to each column of the W matrix:

$$W^{\text{corr}} = W \cdot \text{diag}(-\text{sgn}(\lambda)) \quad (7)$$

After sign correction, $W_{ij}^{\text{corr}} < 0$ represents a signed *marginal improvement* in the LP objective, quantifying a cost-minimizing contribution of MV_i that is economically aligned with the LP objective, regardless of whether CV_j is constrained at the upper or lower bound.

2.4 Local MV-CV Pairing

We can think of classical loop pairing as the ‘forward problem’ for controller synthesis, where we ask which MVs and CVs should be paired together based on process physics and the active constraints we wish to control. In contrast, this LP-MPC pairing framework represents the ‘inverse problem’ for controller diagnostics, where the control strategy has been decided by the LP optimizer based on both process physics and economics. We now want to reverse engineer the LP solution to recover the implicit MV-CV pairings.

For each constrained CV, we define its *locally most effective* MV pair as the choice that yields the greatest improvement in objective function per unit of CV relaxation. This corresponds to the MV row with the most negative entry for each CV column in W^{corr} . However, this local pairing perspective does not account for competition across CVs for the same MV. Since multiple CVs may share the same MV as its locally most effective pair, we must further define a global pairing rule to resolve conflicts and produce a one-to-one MV-CV pairing assignment.

2.5 Scale Invariance for Global MV-CV Pairing

In practice, variables in the gain matrix typically span vastly different engineering units and numerical scales. W^{corr} is scale-dependent with units of $\$/\Delta CV$, making a direct comparison of entries across multiple variables physically not meaningful without appropriate scaling

(Waller and Waller, 1995). To ensure that all shadow price contributions have a common relative basis independent of engineering units, each CV column j is normalized by the absolute value of its most negative element in that column. This choice of CV scaling has several desirable properties. It results in a scale-invariant, dimensionless shadow price contribution matrix Π_{ij} . Each term represents normalized MV contributions to each CV's shadow price on a relative basis, preserving the CV's local ranking of preferred MV pairs in the most negative entry of -1 for each column.

$$\Pi_{ij} = \frac{W_{ij}^{\text{corr}}}{\left| \min_p W_{pj}^{\text{corr}} \right|} \quad (8)$$

Scaling allows us to extend our local pairing definition to a global pairing rule. We define the set of one-to-one *globally most effective* MV-CV pairings as the choice that minimizes the total normalized deviations from each CV's locally most effective MV.

If every CV has a uniquely different local MV pair (i.e. the most negative entry for every CV columns all occur at different MV rows), the global MV-CV pairing rule simply reproduces the set of all local MV-CV pairings. When multiple CVs share the same locally most effective MV, each CV will be assigned to the next-best MV such that the aggregated, normalized deviations are minimized. This global pairing rule allows for tie-breaking across multiple CVs in a consistent manner.

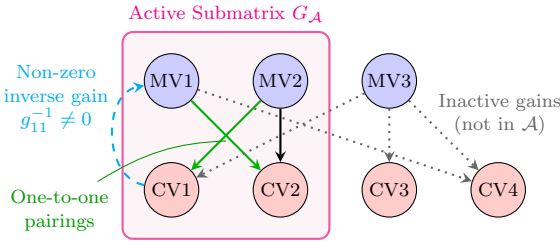


Fig. 4. Visual representation of MV-CV relationships in an LP-MPC controller.

We approach this global pairing rule as a linear sum assignment problem. An assignment penalty matrix $P \in \mathbb{R}^{k \times k}$ encodes the normalized deviation associated with pairing MV_i and CV_j :

$$P_{ij} = \begin{cases} \Pi_{ij}, & |\Pi_{ij}| \neq 0 \\ \infty, & \Pi_{ij} = 0 \end{cases} \quad (9)$$

The locally most effective MV for each CV is $P_{ij} = -1$, which is the smallest possible penalty in the matrix. For a non-existent CV-MV relationship in the inverse gain matrix (i.e. zeros), an infinite penalty of $P_{ij} = \infty$ is assigned to exclude these pairings from consideration. Small penalties $P_{ij} < 0$ encode deviations from the locally most effective MV and represent relative next-best choices for each CV. Larger penalties $P_{ij} > 0$ are due to MV movements that are opposing the shadow price and moving away from the CV constraint, worsening the objective function. These are typically poor choices for pairing but will be selected if all other available MV choices are exhausted.

The penalty matrix P is used as an input to a standard linear sum assignment solver (i.e., the Hungarian algorithm),

which computes the optimal one-to-one assignment that minimizes the total assignment penalty:

$$\begin{aligned} \min_{X \in \{0,1\}^{k \times k}} \quad & \sum_{i=1}^k \sum_{j=1}^k P_{ij} X_{ij} \\ \text{s.t.} \quad & \sum_{i=1}^k X_{ij} = 1, \quad \sum_{j=1}^k X_{ij} = 1 \quad \forall i, j = 1, \dots, k, \end{aligned} \quad (10)$$

The assignment results are expressed using a binary matrix $X \in \{0,1\}^{k \times k}$, where $X_{ij} = 1$ if MV i is assigned to CV j , and 0 otherwise, which yields the globally most effective, minimum-penalty pairings of MVs and CVs, as illustrated by the green arrows in Fig. 4.

3. RESULTS AND DISCUSSION

3.1 Physical Interpretation of MV-CV Pairings

A trivial pairing arises when an MV affects only one CV, or vice-versa. The MV-CV pairing is effectively predetermined since there is only a single choice. In P , if there is a single, unique minima of -1 across both row and column, the MV-CV pairing is also predetermined since any alternative choice would increase the total assignment cost and thus violate optimality in the linear sum assignment solution. These unambiguous pairings can be identified by iteratively removing these rows and columns in P by inspection, even without using an assignment solver. The linear sum assignment algorithm resolves more economically unambiguous pairings, where each CV is assigned to its next-best MV such that the overall deviations from its preferred MV choices are minimized globally.

3.2 Example: 2×2 Square Pairing Problem

Consider an LP-MPC system with gain matrix and LP costs defined as follows.

$$G = \begin{matrix} & \begin{matrix} MV_1 & MV_2 \end{matrix} \\ \begin{matrix} CV_1 \\ CV_2 \\ CV_3 \end{matrix} & \begin{bmatrix} -0.115 & 0.001 \\ 3.090 & 0.080 \\ -0.560 & 0.002 \end{bmatrix} \end{matrix} \quad c^T = [12.5 \ 0.1]$$

We assume that the CV^{ss} starting values are equidistant from the upper and lower CV limits. The effective CV inequality constraints imposed are $-0.7 \leq \Delta CV_1^{ss} \leq 0.7$, $-27 \leq \Delta CV_2^{ss} \leq 27$, $-4 \leq \Delta CV_3^{ss} \leq 4$, with no MV constraints. We can visualize the feasible region and geometry of the solution in terms of incremental MV movements as shown in the left subfigure in Fig. 5. The LP geometry shows that there are 4 possible solutions or vertices in the yellow feasible region, formed by constraints of ΔCV_1^{ss} and ΔCV_2^{ss} .

The inequalities of ΔCV_3^{ss} shown in orange are outside of the feasible region and therefore CV_3^{ss} will not participate in any optimum solution and our subsequent analysis reduces to a 2×2 sub-problem. The angle represented by the cost ratios, $r = (c_2/c_1)$, shown as a blue vector in Fig. 5, determines the direction of optimization and the optimal vertex in MV space. By solving the LP cost minimization problem as described in Eq. (1), the optimum solution is $\Delta MV^* = [-6.8, -76.7]$ found at

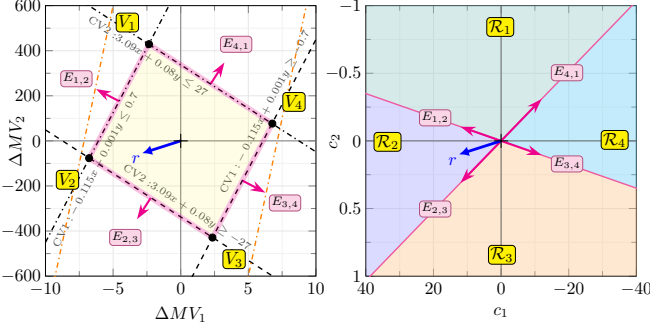


Fig. 5. Left – Feasible region of LP solutions. Right – Normal cones in cost space where each critical region \mathcal{R}_i corresponds to an optimal vertex V_i .

vertex V_2 . What are the MV-CV pairings for this LP solution? The inverse matrix of the active constraint set and corresponding unconstrained MV costs are:

$$G_{\mathcal{A}}^{-1} = \begin{matrix} & CV_1 & CV_2 \\ \begin{matrix} MV_1 \\ MV_2 \end{matrix} & \begin{bmatrix} -6.5094 & 0.0814 \\ 251.4239 & 9.3572 \end{bmatrix} \end{matrix} \quad c_u^T = [12.5 \ 0.1]$$

By Eq. (6) and Eq. (8), adjusting for shadow price signs, $\lambda^T = [-56.22, 1.95]$, we get:

$$W = \begin{matrix} & CV_1 & CV_2 \\ \begin{matrix} MV_1 \\ MV_2 \end{matrix} & \begin{bmatrix} -81.37 & 1.02 \\ 25.14 & 0.94 \end{bmatrix} \end{matrix} \quad W^{\text{corr}} = \begin{matrix} & CV_1 & CV_2 \\ \begin{matrix} MV_1 \\ MV_2 \end{matrix} & \begin{bmatrix} -81.37 & -1.02 \\ 25.14 & -0.94 \end{bmatrix} \end{matrix}$$

After scaling by the magnitude of the most negative entry in each column by Eq. (8), we see that both CVs compete for MV1 as their locally most effective pair since they both have -1 entries in the first row:

$$\Pi = \begin{matrix} & CV_1 & CV_2 \\ \begin{matrix} MV_1 \\ MV_2 \end{matrix} & \begin{bmatrix} -1 & -1 \\ 0.309 & -0.92 \end{bmatrix} \end{matrix}$$

There are only 2 possible pairing choices for this problem.

- Diagonal: $\mathcal{S}_{\text{diag}} = \{MV1 \mapsto CV1, MV2 \mapsto CV2\}$,
- Off-diagonal: $\mathcal{S}_{\text{off}} = \{MV1 \mapsto CV2, MV2 \mapsto CV1\}$.

The total penalties for these two assignments are $P_{\text{diag}} = P_{11} + P_{22}$ and $P_{\text{off}} = P_{12} + P_{21}$. Since $P_{\text{diag}} = -1.92 < P_{\text{off}} = -0.69$, the diagonal pairings will minimize the overall penalty and the optimal set of assignments are $\mathcal{S}_{\text{diag}}^* = \{MV1 \mapsto CV1, MV2 \mapsto CV2\}$.

3.3 Sensitivity Analysis

We perform a sensitivity analysis based on concepts from multiparametric linear programming (mpLP) by sweeping the LP optimum solution as a function of cost ratios, $\Delta MV^*(r)$, as shown in the right subfigure in Fig. 5. Degenerate solutions arise when the cost level sets are parallel to an edge of the feasible region, and either vertex is optimal. Each critical region \mathcal{R}_i represents the cone spanned by the normals of the active constraints at vertex V_i . Within these *normal cones*, the optimal vertex ΔMV^* remains constant, with degenerate solutions at the cone boundaries. What are the switching points where the pairings could flip? They occur when both penalties are equal: $\Delta P = P_{\text{diag}} - P_{\text{off}} = 0$, with $\Delta P < 0$ resulting in a

lower penalty for the diagonal pairing. For this particular problem, by substituting the definitions and values for P when both CVs are competing for the same MV:

$$\Delta P = \frac{c_2}{|c_1|} \left[\frac{[G_{\mathcal{A}}^{-1}]_{21} \text{sgn}(\lambda_1)}{|[G_{\mathcal{A}}^{-1}]_{11}|} - \frac{[G_{\mathcal{A}}^{-1}]_{22} \text{sgn}(\lambda_2)}{|[G_{\mathcal{A}}^{-1}]_{12}|} \right] \quad (11)$$

For any cost ratios within the normal cone of the optimal vertex in Fig. 5, the shadow price sign patterns are fixed, so the bracketed term is constant, and the switching point $\Delta P = 0$ reduces to $c_2 = 0$. If both CVs prefer MV2, by a similar algebraic exercise, $\Delta P = 0$ reduces to $c_1 = 0$. Note that the form of ΔP derived in (11) is only true when the local preferences for MVs are the same. In such cases, pairings will flip when the cost sign changes. This simple analysis shows that even for a 2×2 problem, pairings are not solely determined by the LP optimum, which has important consequences: (1) the optimum is invariant to positive cost scalings if r remains in the same normal cone, (2) the sign patterns of c_1 or c_2 may change the optimum if r moves outside of the normal cone, (3) costs and its sign patterns influence pairings; even when the optimum does not change, pairings may change.

3.4 Visualization of MV-CV Pairings

This MV-CV pairing framework is a practical solution for understanding both real-time and historical controller constraints. When unexpected controller behavior occurs, plant personnel often ‘clamp’ MV limits (less often CV limits) to force the optimizer in certain directions that are operationally desired. This occurs for 3 primary reasons: (1) the objective of the controller is not well understood or the LP solution is counter-intuitive, (2) the economic objectives set by LP costs in the controller are wrong, or (3) gain consistency issues in the model cause the LP to incorrectly trade off constraints (O’Connor et al., 2022). Clamping LP limits can significantly reduce the potential benefits of the application and even result in other non-ideal behaviors that causes operators to switch off the LP-MPC controller.

By comparing pairings from an online controller against ‘ideal’ pairings, practitioners can verify alignment of the controller’s current behaviour with its original design intent. For instance, in a distillation column, bottoms steam flow rate is typically the primary MV for controlling the bottoms product purity CV. In the controller’s original design intent, the ‘ideal’ pairing is steam MV with purity CV. In the online LP solution, if there is a pairing reassignment of the steam MV to another CV such as the column’s differential pressure (dP), it would indicate that the dP limit has hit its upper bound due to flooding or hydraulic limitations. By seeing the pairings reassigned in real-time, operators and engineers would immediately understand why the controller is cutting steam. Practitioners can also leverage historical constraints and pairing data for process improvement opportunities. For instance, by analyzing the fraction of operating time with sub-optimal constraint pairings, e.g. steam paired with an undesirable CV like the column dP, process engineers can estimate the economic benefits of constraint relief. In the short term, this could mean making adjustments to operating practices. In the long term, it can help justify future capital projects.

On an industrial controller (30 MVs, 63 CVs), we extracted the historical square active constraint sets, $\mathcal{A}_1, \mathcal{A}_2, \dots, \mathcal{A}_N$ for an arbitrary 200-day window and evaluated the MV-CV pairings for each control interval. The truncated results (6 of 30 MVs) are presented in Table 1 to conceptually illustrate how to visualize the pairings.

Table 1. Visualization of MV-CV Pairings

	\mathcal{S}_1	\mathcal{S}_2	\mathcal{S}_3	\mathcal{S}_∞
MV2	● CV2-HI (99.4%)	CV3-HI (0.52%)	CV9-HI (0.05%)	● CV7-HI (0.001%)
MV9	● CV12-LO (82.8%)	MV-LO (17.0%)	OOS (0.26%)	
MV13	CV14-HI (96.4%)	CV6-LO (3.2%)	MV-HI (0.43%)	
MV16	MV-LO (55.5%)	● CV17-HI (45.0%)	CV14-HI (0.006%)	
MV17	● MV-LO (96.5%)	OOS (3.5%)	CV14-HI (0.04%)	
MV28	CV4-HI (66.8%)	● CV28-HI (32.1%)	CV27-HI (0.87%)	
Infeasible	● CV4, ● CV10			

Each MV row contains three main columns $\mathcal{S}_1, \mathcal{S}_2, \mathcal{S}_3$ representing the top 3 CV pairings for a given MV row. The pairings are arranged in descending order across each row based on the percentage of time the MV-CV pair was found. For example, MV2 is almost always paired with CV2, 99.4% of the time in the 200 days. For this controller, 3 columns of pairings was enough to cover over 99% of the pairings observed for each of the 30 MVs. The last column \mathcal{S}_∞ is added to highlight unusual pairings not represented by the top 3 pairings, and would typically be blank. The arrangement of this table allows a large number of possible constraint combinations to be displayed in a compact form. This enables personnel to focus on higher-value operational questions like why is MV16 hitting a low limit 55% of the time? Why is MV13 paired with an unusual CV7? Why is MV17 out of service (OOS) 3.5% of the time, or why is MV9 hitting a low MV limit 17% of the time? When MV9 hits a low limit, the controller may have to control CV12 with a less optimal MV.

We superimpose the real time pairings from an online controller as colored dots to the table of historical statistics. This offers an effective visualization approach to analyze the current LP constraints in relation to historical precedence. Green dots indicate ‘ideal’ pairings that match the controller’s design intent. Yellow dots flag ‘non-deal’ pairings for review, implying that the MV is incorrectly clamped or paired with an undesired CV. Note that a clear understanding of the controller’s objectives is needed to determine if a pairing is ‘ideal’. A pairing is considered ‘ideal’ if it aligns with the controller’s design intent, even if it is not the most frequent pair found in \mathcal{S}_1 . Conversely, a historically frequent pairing in \mathcal{S}_1 does not necessarily mean it is ideal. For an infeasible CV represented by a red dot, the historical data in the table would show which MV was paired with it. For situations where the original design intent may be unclear, such as MV17, the historical summary in the table provides a baseline reference for how the controller has typically operated. By reducing the MV17 low limit, it is possible to provide immediate

feedback showing how the MV17 degree of freedom is used in the current environment.

4. CONCLUSIONS

We present an explainable LP-MPC framework based on shadow prices for understanding which MV is primarily driving a CV’s constraint, which represents a novel conceptual leap forward in the search for interpretable LP-MPC controller targets. Our methodology naturally admits multiple valid ways of normalization to construct a dimensionless contribution matrix. Empirically, by evaluating large real-world controllers up to 65 MVs \times 65 CVs, we observed that column normalization based on the largest negative entry resulted in the most consistently ‘correct’ pairings that made engineering sense. However, there is no universally accepted ground truth for these implicit LP-derived MV–CV pairings, which remains an open question for future research. Despite these conceptual limitations, the proposed framework offers practitioners a consistent way to interrogate LP solutions and make the optimizer’s implicit decision-making logic more transparent. The pairing analysis provides valuable diagnostic insights for understanding current and historical controller behavior. Unexpected pairing mismatches can reveal potential controller issues and guide practitioners toward actionable opportunities for constraint relief.

REFERENCES

- Elnawawi, S., Siang, L.C., O’Connor, D.L., and Gopaluni, R.B. (2022). Interactive visualization for diagnosis of industrial model predictive controllers with steady-state optimizers. *Control Eng. Pract.*
- Nikandrov, A. and Swartz, C.L. (2009). Sensitivity analysis of LP-MPC cascade control systems. *J. Process Control*.
- O’Connor, D.L., Siang, L.C., and Elnawawi, S. (2022). A simple discretization scheme for gain matrix conditioning. In *Proc. 7th IEEE AdCONIP Symp.*
- Qin, S.J. and Badgwell, T.A. (2003). A survey of industrial model predictive control technology. *Control Eng. Pract.*
- Siang, L.C., Elnawawi, S., and Steele, D. (2022). Self-service analytics and the processing of hydrocarbons. *Digit. Chem. Eng.*
- Skogestad, S. (2023). Advanced control using decomposition and simple elements. *Annu. Rev. Control*.
- Waller, J.B. and Waller, K.V. (1995). Defining directionality: Use of directionality measures with respect to scaling. *Ind. Eng. Chem. Res.*
- Ying, C.M. and Joseph, B. (1999). Performance and stability analysis of LP-MPC and QP-MPC cascade control systems. *AIChE J.*